A Non-Precious Metal Promoting the Synthesis of 5-Hydroxymethylfurfural

Xinyuan Lu [1], Hongjie Zhao [1], Wei Feng [2],* and Peijun Ji [1],*

[1]   Department of Chemical Engineering, Beijing University of Chemical Technology, Beijing 100029, China; Xinyuanlu209@outlook.com (X.L.); Hongjiezhao420@163.com (H.Z.)
[2]   Department of Biochemical Engineering, Beijing University of Chemical Technology, Beijing 100029, China
*   Correspondence: fengwei@mail.buct.edu.cn (W.F.); jipj@mail.buct.edu.cn (P.J.);
    Tel.: +86-010-64446249 (W.F.); +86-010-64423254 (P.J.)

Abstract: In this work, a new kind of catalyst was prepared for synthesis of 5-hydroxymethylfurfural. Copper ions were incorporated into manganese oxide octahedral molecular sieves (K-OMS-2). The catalysts Cu-K-OMS-2 were characterized by measuring FTIR spectra, scanning electron microscope images, X-ray diffraction patterns, and temperature-programmed desorption (TPD) and temperature-programmed reduction (TPR) profiles. Thermogravimetric analysis (TGA) demonstrated that the stability of Cu-K-OMS-2 is almost the same as that of K-OMS-2. XRD patterns showed that introducing copper ions did not change the structure of K-OMS-2, but copper ions had an effect on the morphology of K-OMS-2 as illustrated by SEM images. TPD profiles demonstrated that both K-OMS-2 and Cu-K-OMS-2 possess basic and acidic sites, and Cu-K-OMS-2 has weak acidic sites. One-pot synthesis of 2,5-diformylfuran (DFF) from fructose was investigated under the catalysis of Cu-K-OMS-2 together with a commercial catalyst Amberlyst 15. The effect of reaction time and temperature on the DFF yield was investigated, and reaction temperature had an effect on the DFF yield. The effect of atomic ratio of Cu to Mn of Cu-K-OMS-2 on the DFF yield was also investigated. The DFF yield was improved 34.7% by Cu-K-OMS-2 in comparison to K-OMS-2, indicating the promotion effect of copper on the DFF yield. Consecutive use of Cu-K-OMS-2 demonstrated that after 6 cycles, the loss of DFF yield was 6.3%, indicating a good reusability of Cu-K-OMS-2.
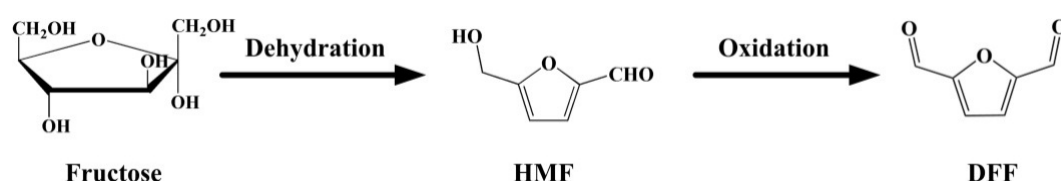
Keywords: 2,5-diformylfuran; OMS-2; copper; synthesis

1. Introduction

2,5-Diformylfuran (DFF) is a value added chemical with broad application prospects. It can be used either as a monomer, or as a starting material for the synthesis of ligands, drugs, and antifungal agents [1]. DFF can be produced by the oxidation of 5-hydroxymethylfurfural (HMF), and HMF can be produced from biomass resource [2]. Considering economy and sustainability, the aerobic oxidation approach to producing DFF from HMF is preferred [3], by using O_2 as oxidant. Developing heterogeneous catalysts has been paid more attention. The goal is to selectively oxidize HMF to DFF. Ruthenium nanoparticles were embedded in mesoporous poly-melamine-formaldehyde, and the conjugate was used for selective oxidation HMF to DFF in solvent toluene [1]. By exchanging Ru^{3+} with H^+ in zirconium phosphate, a ruthenium catalyst was prepared and used for the oxidation of HMF. DFF and 2,5-furandicarboxylic acid (FDCA) were the main components of products [4]. Precious metals present advantages over non-precious metals in preparing heterogeneous catalysts. However, precious catalysts are much expensive. Hence non-precious metals have been investigated for catalyst preparation. Mesoporous manganese doped with cobalt oxide was used for the oxidation of HMF to DFF [5]. Vanadium oxide was embedded in zeolites and used for oxidation of HMF to DFF.

Under the ambient air pressure, the DFF yield of was 83% [6]. Cellulose-mediated Cu nanoparticles were reported for selective oxidation of HMF to DFF [3].

Transformation of carbohydrates into platform chemicals provides an efficient approach to using a biomass resource. As illustrated in Scheme 1, the process involves two steps including fructose dehydration to HMF and oxidation of HMF to DFF. Few studies have reported the DFF synthesis based on a one-pot approach. Starting from fructose, two catalysts were used sequentially, fructose dehydration using an Amberlyst 15 catalyst and the subsequent oxidation of HMF using an Ru-based catalyst, and the DFF yield was 72.4% [7]. The Amberlyst 15 catalyst was used together with hydrotalcite-supported Ruthenium catalysts for the synthesis of DFF [8]. Other catalysts, V_2O_5/ceramic powder catalyst with dilute sulfuric acid [9], magnetic $WO_3HO\text{-}VO\text{-}SiO_2@Fe_3O_4$ with tungstic acid [10], and vanadium oxide [11] have also been reported. High DFF yields are expected from one-pot reaction systems. Developing cost-efficient and environment benign catalytic system for the oxidation of HMF is pursued by researchers.

Scheme 1. Transformation of fructose to 2,5-diformylfuran (DFF) via 5-hydroxymethylfurfural (HMF).

Manganese oxide octahedral molecular sieves (K-OMS-2) exhibit unique structural characteristics, including porous structure, mixed valency for Mn ions (3+ and 4+), and easy release of lattice oxygen. OMS-2 has been explored for preparing catalysts with oxidation functions, and has been used in various systems. The addition of metal ions to K-OMS-2 is a solution to improving its catalytic capability. Transition metal cations and alkali were used to replace K^+ in the tunnel. The cations have been found to be mobile and can stabilize the structure of the nodule. Some cations can be incorporated into the framework. The cation K^+ in K-OMS-2 was substituted with Ag^+ in the K-OMS-2, resulting in the formation of Ag-OMS-2, which had been shown as an efficient oxidation catalyst. In this work, copper ions were incorporated into K-OMS-2 for selective oxidation HMF to DFF. One-pot DFF synthesis from fructose under the catalysis of Cu-K-OMS-2 and a commercial catalyst Amberlyst 15 was studied.

2. Results and Discussion

2.1. Characterization of the Cu-K-OMS-2 Catalysts

K-OMS-2 was prepared by adding $KMnO_4$ to the solution of $MnSO_4 \cdot H_2O$ in concentrated HNO_3. A serious of Cu-K-OMS-2 were prepared by adding $KMnO_4$ to the solution of $MnSO_4 \cdot H_2O$ and $Cu(NO_3)_2 \cdot 3H_2O$ in concentrated HNO_3. Cu-K-OMS-2-I, Cu-K-OMS-2-II, and Cu-K-OMS-2-III represent the catalysts prepared with different ratios of Cu to Mn in the catalysts as shown in Table 1. The bulk contents of copper and manganese of the samples were determined by ICP-AES.

Table 1. Atomic ratios of Cu to Mn in the catalysts.

Catalysts	Cu/Mn (Atomic Ratio)
K-OMS-2	0
Cu-K-OMS-2-I	0.019
Cu-K-OMS-2-II	0.024
Cu-K-OMS-2-III	0.031

2.1.1. Scanning Electron Microscope Images

Figure 1 shows the scanning electron microscope (SEM) images for K-OMS-2 and Cu-K-OMS-2. Compared to the SEM image of K-OMS-2 (Figure 1a), Cu-K-OMS-2-I exhibited dense microsize particles. Cu-K-OMS-2-II exhibited particles larger than K-OMS-2 and Cu-K-OMS-2-I. K-OMS-2, Cu-K-OMS-2-I, and Cu-K-OMS-2-III exhibited spherical particles. In contrast, Cu-K-OMS-2-III exhibited shuttle-like particles. Figure 1 shows that the existence of Cu affected the morphology of the catalysts.
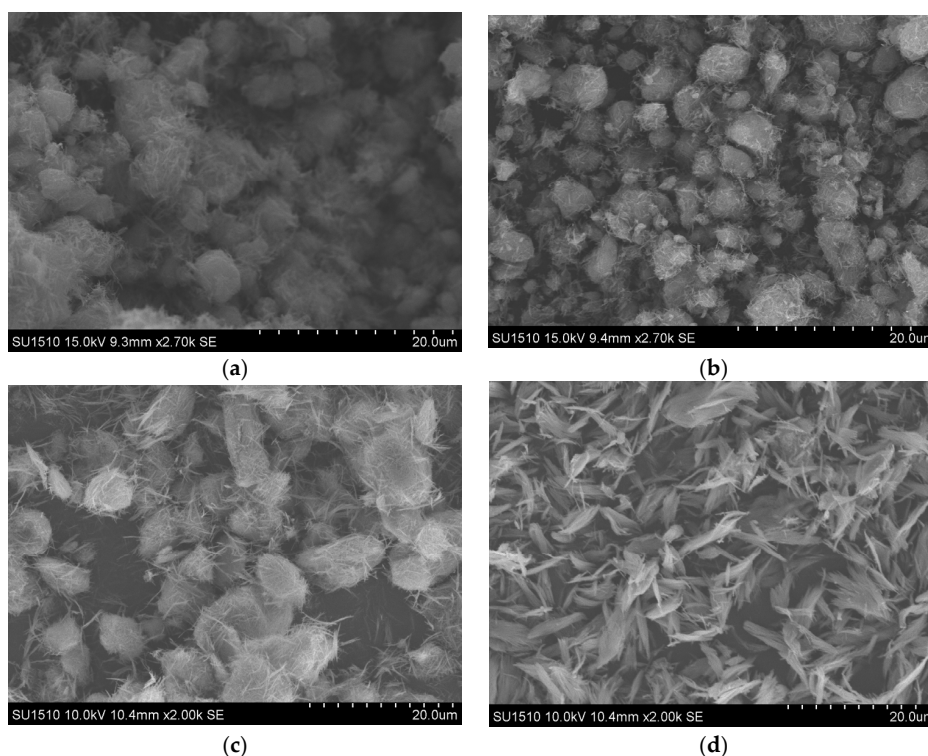

(a)　　　　(b)

(c)　　　　(d)

Figure 1. SEM images. K-OMS-2 (**a**); Cu-K-OMS-2-I (**b**); Cu-K-OMS-2-II (**c**); Cu-K-OMS-2-III (**d**).

2.1.2. Spectra of Fourier Transform Infrared Spectoscopy

K-OMS-2 and Cu-K-OMS-2 were further characterized by Fourier transform infrared spectroscopy (FTIR), as shown in Figure 2. The three bands at 720, 525, and 470 cm^{-1} were attributed to Mn–O and Cu–O vibrations [12,13]. The FTIR spectra show that the existence of Cu did not shift the band position. When the ratio of Cu to Mn was increased, the band intensity at 470 cm^{-1} increased. The FTIR spectra confirmed the existence of Cu in K-OMS-2.
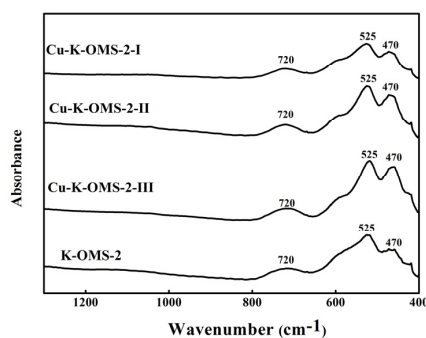

Figure 2. FTIR spectra of K-OMS-2, Cu-K-OMS-2-I, Cu-K-OMS-2-II, and Cu-K-OMS-2-III.

2.1.3. X-ray Diffraction (XRD) Patterns

The X-ray diffraction (XRD) patterns for the catalysts of K-OMS-2, Cu-K-OMS-2-I, Cu-K-OMS-2-II, and Cu-K-OMS-2-III are shown in Figure 3. The X-ray diffraction patterns of K-OMS-2 catalysts are in good agreement with the standard pattern of pure cryptomelane. The synthesized OMS-2 exhibited typical peaks at 12.74°, 18.06°, 28.74°, 37.62°, 42.03°, 49.90°, 56.18°, 60.24°, and 65.52°. These peaks are in consistent with the K-OMS-2 standard card (JCPDS file #29-1020). All peaks can be indexed to a pure cryptomelane phase (JCPDS 29-1020), and no other phases appeared (Figure 3a). The XRD patterns of Cu-K-OMS-2-I, Cu-K-OMS-2-II, and Cu-K-OMS-2-III match well with cryptomelane, and no additional phases appeared for the Cu doped materials (Figure 3b–d). Thus, Cu ions were incorporated well in birnessite without causing apparent disorder to the structure of K-OMS-2.
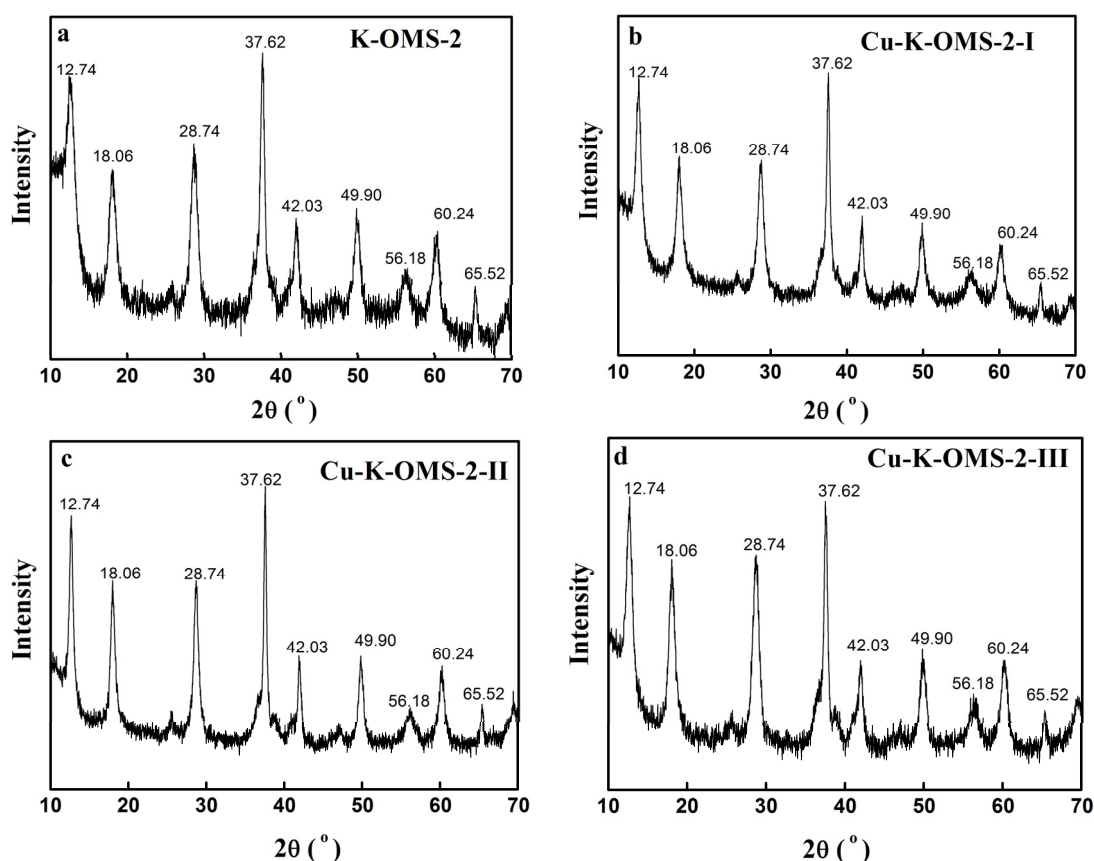

Figure 3. XRD patterns for K-OMS-2 (**a**), Cu-K-OMS-2-I (**b**), Cu-K-OMS-2-II (**c**), and Cu-K-OMS-2-III (**d**).

2.1.4. Thermogravimetric Analysis

The thermal stability of the catalysts was analyzed via thermogravimetric analysis (TGA) measurements as shown in Figure 4. The weight loss versus temperature profiles demonstrate that Cu-K-OMS-2-II exhibited almost the same stability as that of K-OMS-2. The weight losses were in the following regions: 30–280 °C, 280–450 °C, and 570–700 °C. The weight loss from 30 to 280 °C were attributed to adsorbed water and carbon dioxide. The slight weight loss from 280 to 450 °C was ascribed to the chemisorbed oxygen. The weight losses in the 570–700 °C region were ascribed to the collapse of OMS-2 and the decomposition of manganese oxides [14].
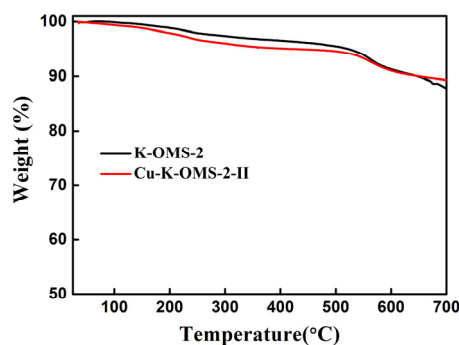
Figure 4. Thermogravimetric analysis (TGA) profiles, weight loss versus temperature, for K-OMS-2 and Cu-K-OMS-2-II.

2.1.5. Temperature-Programmed Desorption

Temperature-programmed desorption (TPD) analysis was shown in Figure 5, with carbon dioxide as probe molecule. The profile confirmed that both K-OMS-2 and Cu-K-OMS-2 possess basic and acidic sites. The basic sites are provided by Mn^{4+}. Figure 6 shows the TPD analysis with ammonia as probe molecule. Both K-OMS-2 and Cu-K-OMS-2-II have acidic sites on their surfaces, and the desorption peaks at around 220 and 130 °C were ascribed to the strong and weak acidic sites, respectively. Cu-K-OMS-2-II has weak acidic sites. Addition of Cu into K-OMS-2 decreases the acidic sites.
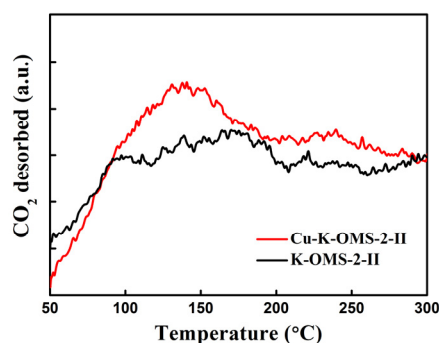

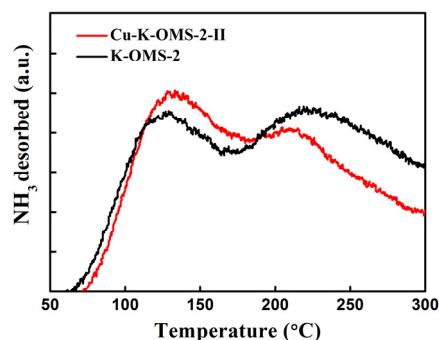**Figure 5.** CO_2-TPD profiles of K-OMS-2 and Cu-K-OMS-2-II. TPD: temperature-programmed desorption.

Figure 6. NH_3-TPD profiles of K-OMS-2 and Cu-K-OMS-2-II.

2.1.6. Temperature-Programmed Reduction

To investigate the stability of the catalyst and effect of oxidation and reduction cycle on the stability, Temperature-programmed reduction (TPR) was carried out twice. Figure 7 shows that there was no major change in the TPR profile of Cu-K-OMS-2-II compared to that of K-OMS-2. The presence

of copper increases the weak acidity as shown in Figures 5 and 6 for the CO_2 and NH_3 profiles, respectively. Figure 7 shows that the presence of copper reduced the reduction temperature about 5 °C. Thus, the reduction and oxidation cycle does not change the structure of the catalyst.
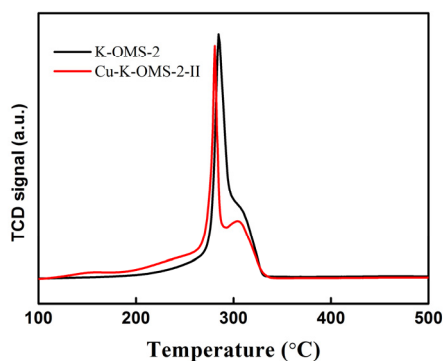

Figure 7. Temperature-programmed reduction (TPR) profiles of K-OMS-2 and Cu-K-OMS-2-II.

2.2. DFF Synthesis

Figure 8 shows the HMF yield from the fructose dehydration reaction under the catalysis of Amberlyst 15. Reaction time and temperature affected the HMF yield. Comparison between 30 and 60 min reaction time, the difference in HMF yield is not significant. In contrast, the effect of reaction temperature is more prominent. At 160 °C, about 90% of HMF yield were obtained after 30 min. The catalysts Cu-K-OMS-2 were used together with a commercial catalyst Amberlyst 15 for one-pot catalysis, converting fructose to DFF.
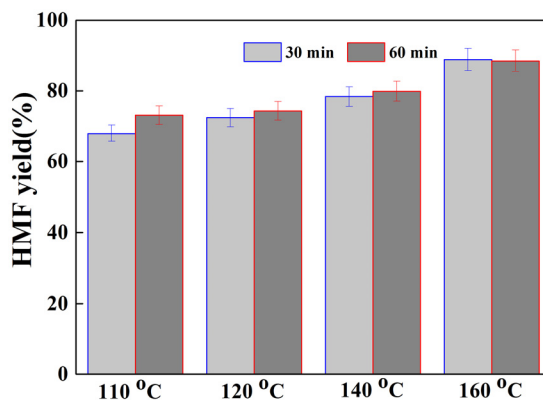

Figure 8. HMF yield as a function of reaction temperature under the catalysis of Amberlyst 15.

Figure 9 illustrates the DFF yield under the catalysis of Amberlyst 15 and different OMS-2 catalysts. The results demonstrated that Cu-K-OMS-2-II achieved the highest DFF yield, indicating that Cu-K-OMS-2-II has a better catalysis ability than Cu-K-OMS-2-I and Cu-K-OMS-2-III. For further investigations of one-pot catalysis, the catalysis using Cu-K-OMS-2-II together with Amberlyst 15 was studied.
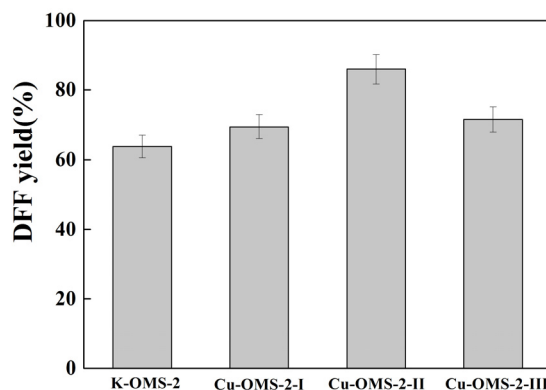
Figure 9. DFF yield under the catalysis of Amberlyst 15 and Cu-K-OMS-2. Reaction time and temperature were 12 h and 160 °C, respectively.

Figure 10 shows the effect of reaction temperature on the DFF yield. With increasing reaction temperature, the DFF yield increased and the HMF yield decreased. The results in Figure 10 demonstrate that the reaction is intrinsically kinetically controlled. Figure 11 shows the profiles of DFF and HMF yields versus reaction time under the catalysis of Amberlyst 15 and Cu-K-OMS-2-II. The reaction temperature was 160 °C. Due to the continuous conversion of HMF to DFF, the DFF yield increased with reaction time, while the HMF yield decreased with the reaction time. After 12 h, the DFF yield reached the highest values.
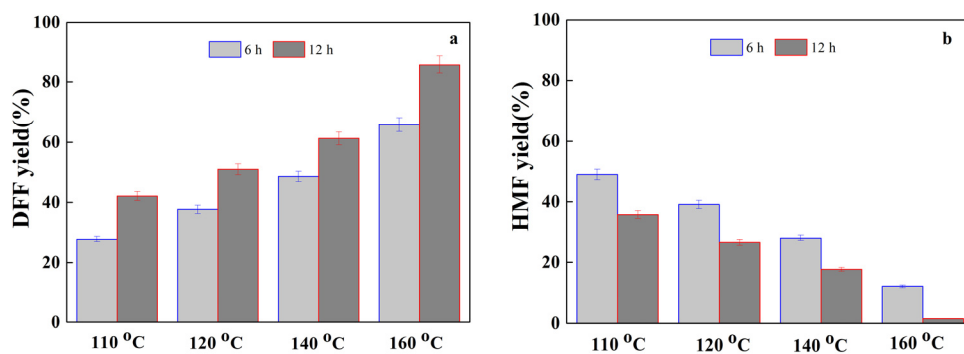

Figure 10. DFF yield (**a**) and HMF yield (**b**) as a function of reaction temperature under the catalysis of Amberlyst 15 and Cu-K-OMS-2-II.
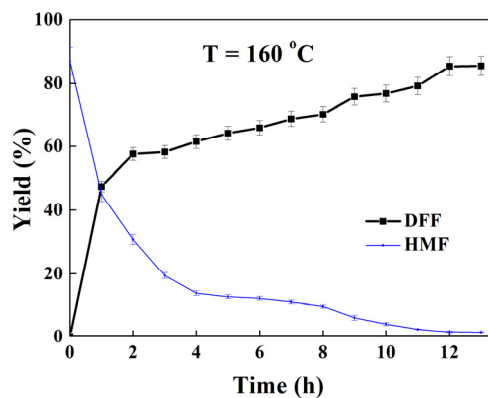

Figure 11. DFF and HMF yields versus reaction time under the catalysis of Amberlyst 15 and Cu-K-OMS-2-II.

Figure 12 shows the consecutive use of Cu-K-OMS-2-II together with Amberlyst 15 for the conversion of fructose to DFF. After 6 cycles of reuse of the catalysts, the loss of DFF yield was 6.3%, indicating a good reusability of Cu-K-OMS-2-II. The catalysis results demonstrated that incorporating copper ions into K-OMS-2 leading to improved catalysis capability for synthesizing DFF. This is due to a significant enhancement of the lattice oxygen activity in K-OMS-2 arising from the Cu ion-substituted K-OMS-2 structure with Mn vacancies. In addition, the presence of Cu^{2+} ions decreases the Mn^{2+}/Mn^{4+} ratio in Cu-K-OMS-2 and increases the average oxidation state of Mn [14].
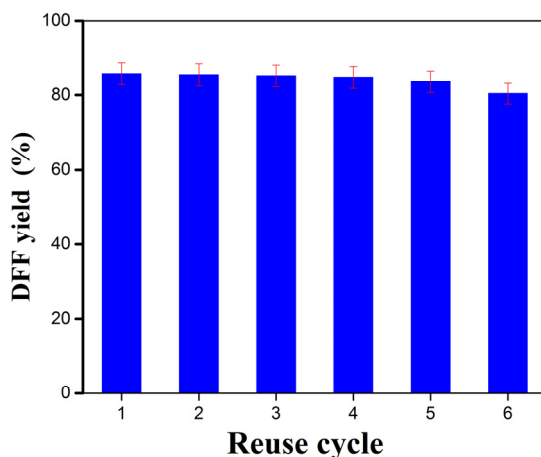

Figure 12. Consecutive use of Cu-K-OMS-2-II for synthesis of DFF.

3. Experimental Section

3.1. Materials

The chemicals required for the synthesis of catalyst and catalytic reactions were purchased from Sigma-Aldrich (Shanghai, China) or Sinopharm Chemical Reagent Co., Ltd (Shanghai, China) and used as received without further purification.

3.2. Catalyst Synthesis

Preparation of K-OMS-2. K-OMS-2 was synthesized by the reflux method [15–18]. The $KMnO_4$ solution (44.3 mg/mL) was added to a mixture of $MnSO_4 \cdot H_2O$ solution (66 mg/mL) and concentrated HNO_3 (1.36 mL). The suspension was stirred vigorously and refluxed at 100 °C for 20 h. After filtration, the precipitate was washed with distilled water until neutral pH and dried at 120 °C for 6 h.

Preparation of Cu-K-OMS-2. $KMnO_4$ solution (44.3 mg/mL) was added to a mixture of $MnSO_4 \cdot H_2O$ solution (66 mg/mL), $Cu(NO_3)_2 \cdot 3H_2O$ (11.8, 23.6 or 35.4 mg/mL), and concentrated HNO_3 (1.36 mL). The suspension was stirred vigorously and refluxed at 100 °C for 20 h. After filtration, the precipitate was washed with distilled water until neutral pH and dried at 120 °C for 6 h.

3.3. Aerobic Oxidation of HMF

An amount of 0.36 g of fructose was dissolved in 10 mL of DMSO. Then, Amberlyst-15 (0.2 g) and Cu-K-OMS-2 (0.4 g) were added to the solution. The mixture was heated under stirring. The mixture was mechanically stirred for 30 min, and oxygen was then introduced into the system from the bottom at a flow rate of 20 mL·min^{-1}. The reaction was carried out for 13 h. After reaction, the catalyst was collected, washed, and dried under vacuum (45 °C) for the next recycling reaction.

HMF, DFF, and intermediates were monitored using HPLC (Shimadzu 15 LC-10A, Shanghai, China) with a Zorbax Eclipse XDB-C8 column (Agilent, Beijing, China) as in our previous work [19]. The mobile phase consisting of phosphate buffer (12 mM, pH 7.0) and acetonitrile was flowed into the system at a flow rate of 1.4 mL·min^{-1}. After 1.6 min of phosphate buffer flowing, the flow rate

of acetonitrile was increased to 5% in 5.0 min and subsequently to 40% in 3 min. After 0.5 min of acetonitrile flowing, phosphate buffer was used as the eluent and maintaining the state for 2 min. Detection was carried out at 268 nm.

3.4. Characterization

Infrared spectra were recorded on a Bruker Tensor 27 FTIR spectrometer (BRUKER, Beijing, China) at a resolution of 2 cm^{-1}. The XRD patterns were obtained with a powder diffractometer of X'Pert PRO MPD (EPCO, Shanghai, China). The powder diffractograms were scanned at a rate of 1°/min from 5° to 90°. The morphology of Cu-K-OMS-2 and K-OMS-2 was observed by scanning electron microscope (SEM) (TESCAN, Shanghai, China) images. Cu cation loaded in K-OMS-2 was analyzed with inductively coupled plasma-atomic emission spectroscopy (ICP-AES) (Thermo Fisher Scientific, Beijing, China). Thermogravimetric analyses (TGA) (Innuo, Shanghai, China) were carried out with a High TGA 2950 Thermalgravimetric Analyzer with a 60 mL/min N$_2$. The temperature was from 25 to 700 °C at a heating rate of 20 °C/min [20].

4. Conclusions

Copper ions were incorporated into K-OMS-2. The catalysts Cu-K-OMS-2 exhibited almost the same stability as that of K-OMS-2. Introducing copper ions did not change the structure of K-OMS-2, but copper ions had an effect on the morphology of K-OMS-2. Both K-OMS-2 and Cu-K-OMS-2 possess basic and acidic sites, and Cu-K-OMS-2 has weak acidic sites. One-pot synthesis of 2,5-diformylfuran (DFF) from fructose was investigated under the catalysis of Cu-K-OMS-2 together with a commercial catalyst Amberlyst 15. Reaction temperature had an effect on the DFF yield. The atomic ratio of Cu to Mn of Cu-K-OMS-2 also affects the DFF yield. The DFF yield has been improved 34.7% by Cu-K-OMS-2 in comparison to K-OMS-2, indicating the promotion effect of copper on the DFF yield. Consecutive use of Cu-K-OMS-2 demonstrated that, after 6 cycles, the loss of DFF yield was 6.3%, indicating a good reusability of Cu-K-OMS-2.

Author Contributions: Peijun Ji and Wei Feng provided the idea for the study; Xinyuan Lu and Hongjie Zhao performed the experiments; Xinyuan Lu and Hongjie Zhao drafted the manuscript; Peijun Ji and Wei Feng revised it.

Conflicts of Interest: The authors declare no conflict of interest.

References

1. Ghosh, K.; Molla, R.A.; Asif Iqubal, M.; Safikul Islam, S.; Manirul Islam, S. Ruthenium nanoparticles supported on N-containing mesoporous polymer catalyzed aerobic oxidation of biomass-derived 5-hydroxymethylfurfural (HMF) to 2,5-diformylfuran (DFF). *Appl. Catal. A* **2016**, *520*, 44–52. [CrossRef]
2. Jérôme, F.; Vigier, K.D.O. catalytic conversion of carbohydrates to furanic derivatives in the presence of choline chloride. *Catalysts* **2017**, *7*, 218. [CrossRef]
3. Baruah, D.; Hussain, F.L.; Suri, M.; Saikia, U.P.; Sengupta, P.; Dutta, D.K.; Konwar, D. Bi(NO$_3$)$_3$·5H$_2$O and cellulose mediated Cu-NPs—A highly efficient and novel catalytic system for aerobic oxidation of alcohols to carbonyls and synthesis of DFF from HMF. *Catal. Commun.* **2016**, *77*, 9–12. [CrossRef]
4. Wang, F.; Yuan, Z.; Liu, B.; Chen, S.; Zhang, Z. Catalytic oxidation of biomass derived 5-hydroxymethylfurfural (HMF) over RuIII-incorporated zirconium phosphate catalyst. *J. Ind. Eng. Chem.* **2016**, *38*, 181–185. [CrossRef]
5. Biswas, S.; Dutta, B.; Mannodi-Kanakkithodi, A.; Clarke, R.; Song, W.; Ramprasad, R.; Suib, S.L. Heterogeneous mesoporous manganese/cobalt oxide catalysts for selective oxidation of 5-hydroxymethylfurfural to 2,5-diformylfuran. *Chem. Commun.* **2017**, *53*, 11751–11754. [CrossRef] [PubMed]
6. Grasset, F.L.; Katryniok, B.; Paul, S.; Nardello-Rataj, V.; Pera-Titus, M.; Clacens, J.M.; De Campof, F.; Dumeignil, F. Selective oxidation of 5-hydroxymethylfurfural to 2,5-diformylfuran over intercalated vanadium phosphate oxides. *RSC Adv.* **2013**, *3*, 9942–9948. [CrossRef]

7. Wang, W.; Jiang, L.; Wang, J.; Zhang, Z. Catalytic conversion of fructose and 5-hydroxymethylfurfural into 2,5-diformylfuran over SBA-15 supported ruthenium catalysts. *Energy Fuels* **2016**, *30*, 5885–5892. [CrossRef]

8. Takagaki, A.; Takahashi, M.; Nishimura, S.; Ebitani, K. One-pot synthesis of 2,5-diformylfuran from carbohydrate derivatives by sulfonated resin and hydrotalcite-supported ruthenium catalysts. *ACS Catal.* **2011**, *1*, 1562–1565. [CrossRef]

9. Cui, M.; Huang, R.; Qi, W.; Su, R.; He, Z. Cascade catalysis via dehydration and oxidation: One-pot synthesis of 2,5-diformylfuran from fructose using acid and V_2O_5/ceramic catalysts. *RSC Adv.* **2017**, *7*, 7560–7566. [CrossRef]

10. Mittal, N.; Nisola, G.M.; Malihan, L.B.; Seo, J.G.; Kim, H.; Lee, S.P.; Chung, W.J. One-pot synthesis of 2,5-diformylfuran from fructose using a magnetic bi-functional catalyst. *RSC Adv.* **2016**, *6*, 25678–25688. [CrossRef]

11. Halliday, G.A.; Young, R.J.; Grushi, V. One-pot, two-step, practical catalytic synthesis of 2,5-diformylfuran from fructose. *Org. Lett.* **2003**, *5*, 2003–2005. [CrossRef] [PubMed]

12. Shyam, P.; Chaturvedi, S.; Karmakar, K.; Bhattacharya, A.; Singh, S.; Kulkarni, S. Structural and magnetic investigations on a wet chemically synthesized nanoscale S = 1/2 spin chain compound—$CuSe_2O_5$. *J. Mater. Chem. C* **2016**, *4*, 611–621. [CrossRef]

13. Rowsell, J.L.C.; Taylor, N.J.; Nazar, L.F. Structure and ion exchange properties of a new cobalt borate with a tunnel structure "templated" by Na^+. *J. Am. Chem. Soc.* **2002**, *124*, 6522–6523. [CrossRef] [PubMed]

14. Wang, R.; Li, J. Effects of precursor and sulfation on OMS-2 catalyst for oxidation of ethanol and acetaldehyde at low temperatures. *Environ. Sci. Technol.* **2010**, *44*, 4282–4287. [CrossRef] [PubMed]

15. Kumara, R.; Sithambarama, S.; Suibabc, S.L. Cyclohexane oxidation catalyzed by manganese oxide octahedral molecular sieves—Effect of acidity of the catalyst. *J. Catal.* **2009**, *262*, 304–313. [CrossRef]

16. Iyer, A.; Galindo, H.; Sithambaram, S.; Merker, T.; Schleid, T.; Hasse, H.; Gläser, R. Nanoscale manganese oxide octahedral molecular sieves (OMS-2) as efficient photocatalysts in 2-propanol oxidation. *Appl. Catal. A* **2010**, *375*, 295–302. [CrossRef]

17. Schurz, F.; Bauchert, J.M.; Merker, T.; Schleid, T.; Hasse, H.; Gläser, R. Octahedral molecular sieves of the type K-OMS-2 with different particle sizes and morphologies: Impact on the catalytic properties in the aerobic partial oxidation of benzyl alcohol. *Appl. Catal. A* **2009**, *355*, 42–49. [CrossRef]

18. Deguzman, R.N.; Shen, Y.; Neth, E.J.; Suib, S.L.; O'Young, C.; Levine, S.; Newsam, J.M. Synthesis and characterization of octahedral molecular sieves (OMS-2) having the hollandite structure. *Chem. Mater.* **1994**, *6*, 815–821. [CrossRef]

19. Gong, W.; Zheng, K.; Ji, P. Platinum deposited on cerium coordination polymer for catalytic oxidation of hydroxymethylfurfural producing 2,5-furandicarboxylic acid. *RSC Adv.* **2017**, *7*, 34776–34782. [CrossRef]

20. Glover, D.; Schumm, B., Jr.; Kozowa, A. (Eds.) *Handbook of Manganese Dioxides Battery Grade*; International Battery Materials Association: Paris, France, 1989.